*Supporting Information*

# Determination of dissociation constants via quantitative mass spectrometry

**Table of Contents**

Materials and Methods

## Protein production

Murine extended Roquin E212A (89-404) was expressed and purified as described before(Tants *et al.*, 2022). Briefly, the protein was expressed from a pETM11 vector as a 6xHis-thioredoxin-fusion construct overnight at 37°C. Cells were collected by centrifugation and lysed by sonication. After a first IMAC, the protein was TEV-digested overnight at 4°C and subsequently passed through a reverse IMAC. For polishing the protein was purified by SEC (SD75 16/600 from GE®), buffer exchanged to 20 mM NaCl, 20 mM Tris pH 7.0, 2 mM TCEP and stored at -80°C.

## RNA production

Both ADE and LBE were produced by *in vitro* transcription. The ADE was transcribed from a HDV-containing plasmid, for the LBE a linear oligo was used and annealed to a T7 top strand (TAATACGACTCACTATA) as template. Transcriptions were performed as described before(Tants *et al.*, 2022). RNAs were purified on a 14% (ADE) and 20% (LBE) denaturing urea PAGE. After excission of target bands RNAs were eluted by crush-and-soak and buffer exchanged to 20 mM NaCl, 20 mM Tris pH 7.0, 2 mM TCEP using an Amicon® centrifugal filter unit. The ADE was refolded by snap cooling and the LBE was denatured at 95°C for 5 min and slowly cooled down at room temperature. RNAs were stored at -80°C.

## DNA preparation

All ssDNA strands were were purchased as desalted, dry custom oligonucleotides from Thermo Fisher Scientific. The corresponding DNA pairs (**Supplementary Table 1**) were solved with a concentration of 10 µM each in a 0.5 mM $MgHPO_4$ buffer with a pH of 7.2. Prior to measurements the sample was annealed at 95 °C for 10 min before cooling to room temperature over several hours.

## NMR spectroscopy

Structural integrity of RNAs was confirmed by NMR spectroscopy. $^{1}H$ imino proton spectra were recorded at 293 K on a 800 MHz Bruker AV equipped with a triple-resonance cryoprobe. Spectra were compared to previous results [1, 2] and confirm duplex formation and linearity of ADE and LBE, respectively, through detection or absence of imino resonances (**Supplementary Figure 1A**).

## Electrophoretic mobility shift assay

ADE and LBE RNAs were 5'-end labelled with [γ-$^{32}P$]-ATP as described before (Tants *et al.*, 2022). RNAs were incubated with increasing amounts of extROQ (0; 50 ; 100; 200; 300; 400; 500; 600; 700; 1,000; 1,500; 2,000; 5000; 10,000; 20,000 nM for the ADE; 0; 50; 100; 200; 300; 500; 750; 1,000; 2,500; 5,000; 10,000; 15,000; 20,000; 25,000; 30,000 nM for the LBE) for 20 min at room temperature. Complexes were separated on native polyacrylamide gels which were run at 4°C and 80 V for 80 min (6% for ADE complexes, 8% for LBE complexes). Dried gels were image with a Typhoon 9400 Variable Mode Imager (GE). Gel bands were quantified as described before (Tants *et al.*, 2022) and calculation of $K_D$s was performed accordingly.

## LILBID laser dissociation curves

LILBID-MS spectra were measured at room temperature using a home-built mass spectrometer with a LILBID ion source and ToF detector, as described in the main article. Droplets of the aqueous sample are emitted from a glass capillary with a 30 µm wide nozzle. These are transferred into a vacuum of about $10^{-5}$ mbar and irradiated by a 2.8 µm laser pulse of about 6 ns in pulse width. This leads to a rapid expansion of the droplet during which ions from the sample are transferred into the gas phase and analysed by their m/z ratio. The resulting plume is illuminated 5 µs after the IR laser pulse by a Minilite I laser (Continuum, San Jose, USA) with a pulse width of ca. 6 ns and recorded by a DFK 23UP031 camera (Imaging Source, Bremen, Germany). With this setup for each droplet a mass spectrum and a picture of the corresponding plume was taken. The size of the plume (explosion width) was evaluated by Fiji.

The percentage of dissociation was calculated as the peak area of the singly charged protein or singly charged 35mer divided by the sum of the singly charged complex or the singly charged dsDNA and the protein or 35mer respectively. For further information regarding this calculation of peak areas of the oligonucleotides, the reader is referred to (Young *et al.*, 2020). These peak areas were evaluated with OriginPro 2020. Due to a stronger peak overlap in the ROQ and LBE system, a Pearson VII fit has been done for a protein only sample to approximate the peak form. The resulting parameters have been used to fit all peaks and to derive the peak areas for the RNA binding protein systems.

## Supplementary Figures

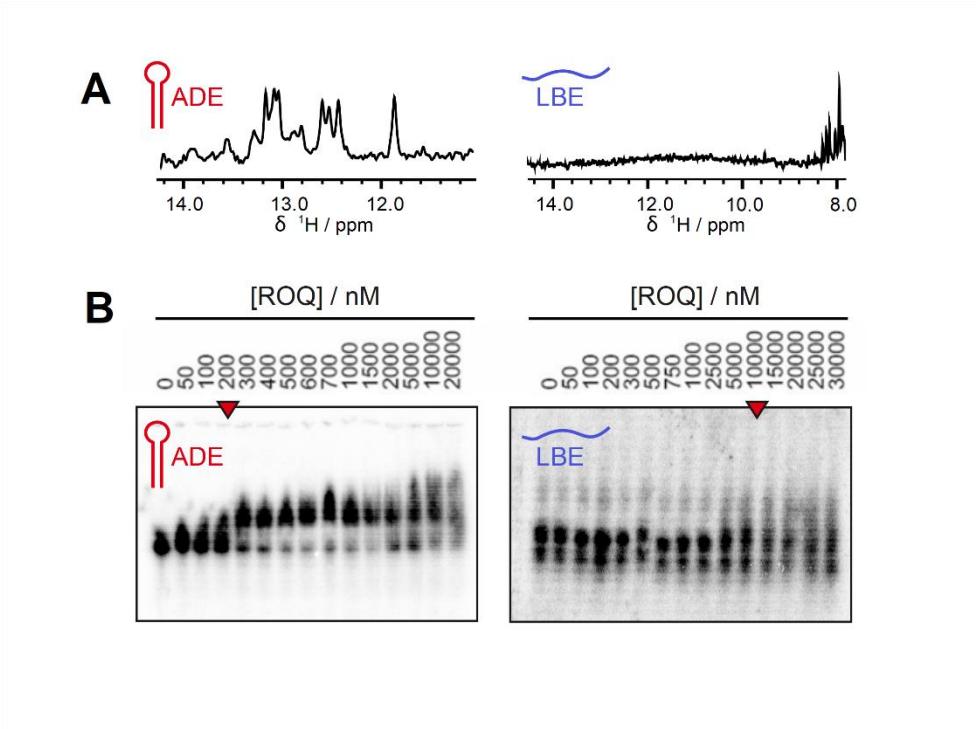


**Supplementary Figure 1: Affinity of extROQ vs. ADE or LBE determined by EMSAs.** **A** 1D $^{1}$H imino proton spectra of ADE and LBE. **B** EMSA of extROQ and ADE or LBE. Red arrows indicate KD points. Previous studies have shown nanomolar binding of extROQ to the *Ox40* ADE (Tants *et al.*, 2022)and low micromolar binding to the *Nfκbid* LBE (Essig *et al.*, 2018). The shown EMSAs at 20 mM NaCl concentrations confirmed these results.

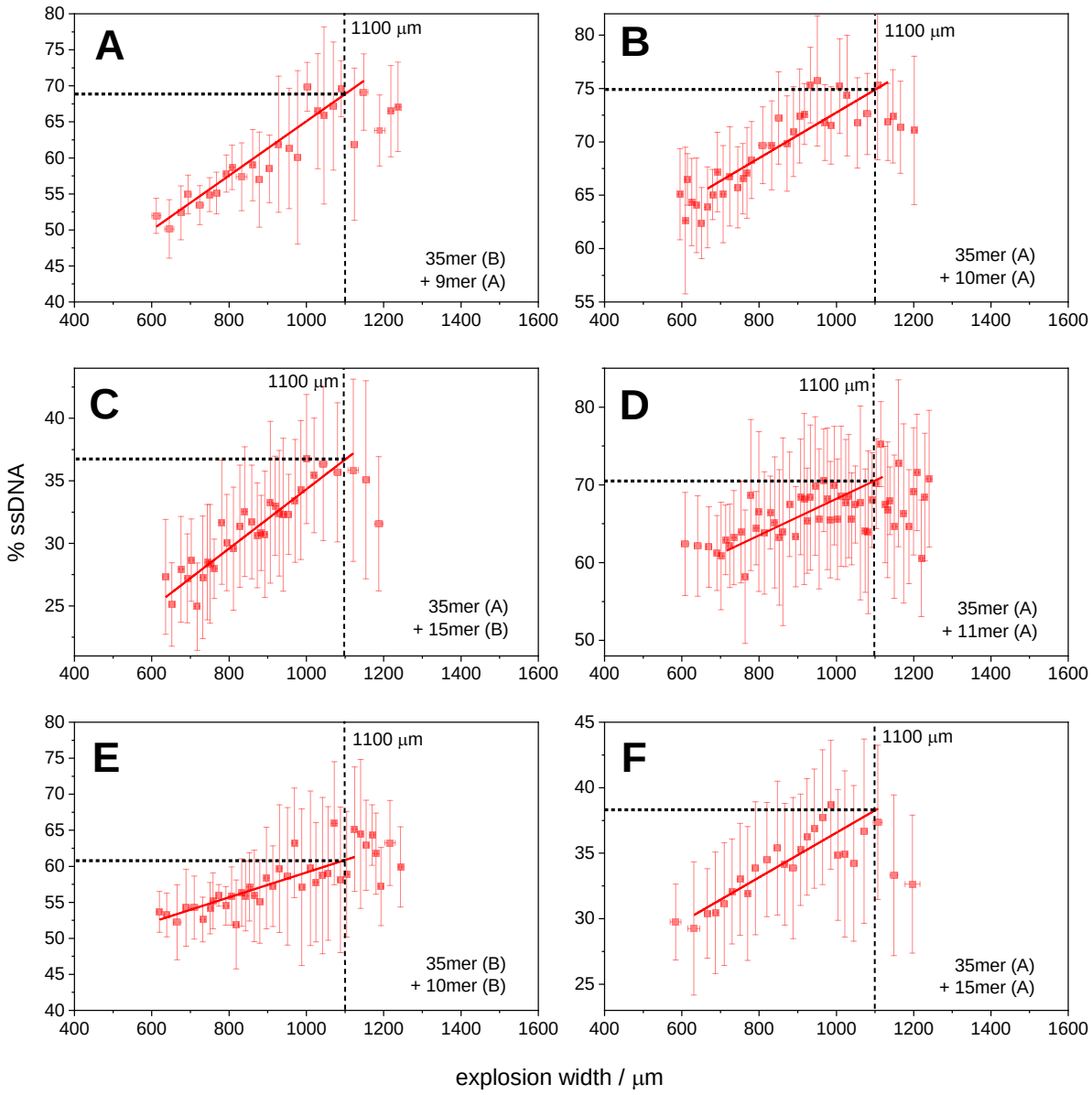


**Supplementary Figure 2: Dissociation curves of dsDNA for the calibration**
Dissociation curves of **A** 35mer (B) and 9mer (A), **B** 35mer (A) and 10mer (A), **C** 35mer (A) and 15mer (B), **D** 35mer (A) and 11mer (A), **E** 35_35mer (B) and 10mer (B), **F** 35mer (A) and 15mer (A). For the sake of legibility one exemplary dissociation curve is shown. Resulting fit parameters and percentage of dissociated double strand at 1100 µm explosion width are given in **Supplementary Table 2**.

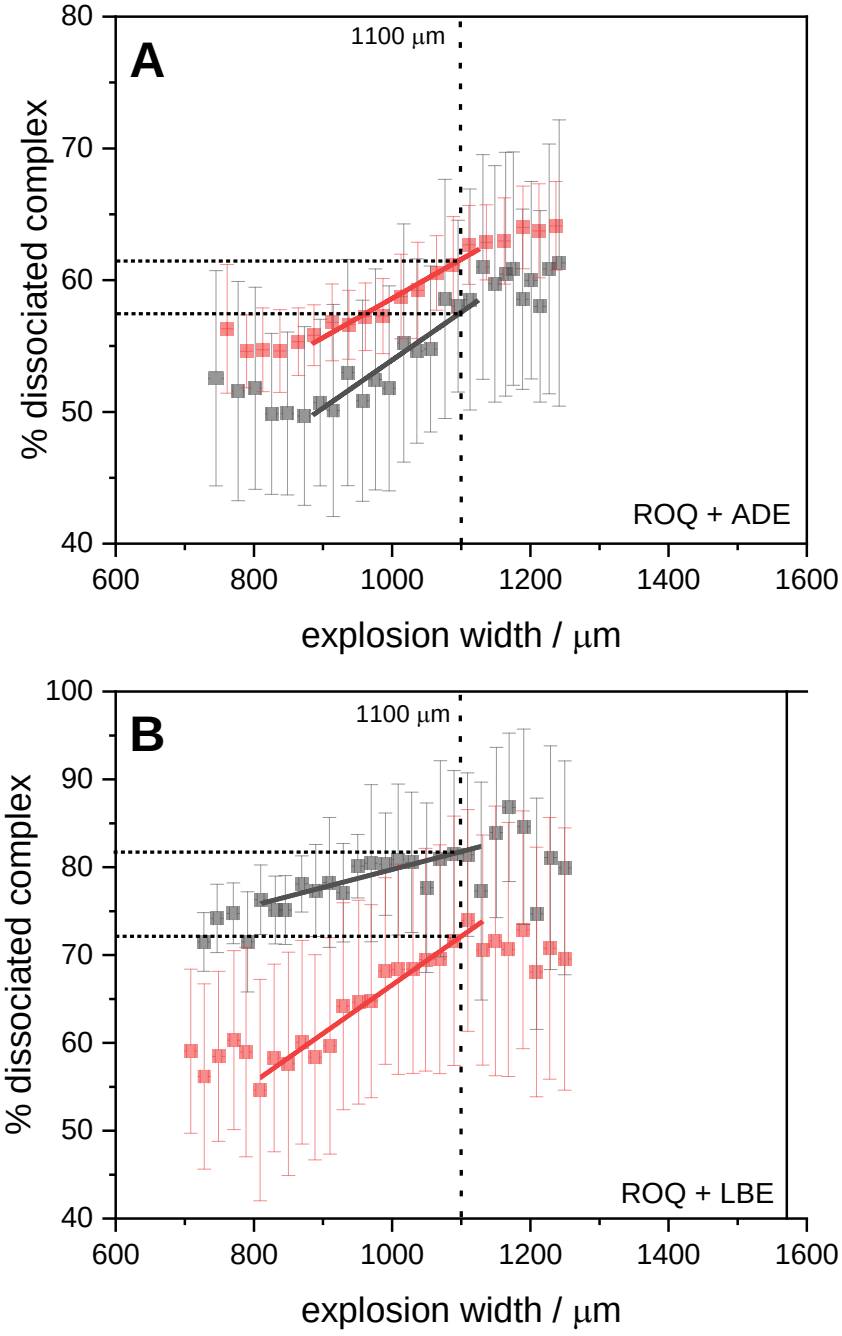


**Supplementary Figure 3: Dissociation curves of RNA binding protein systems**
Disssociation curves of coreROQ with ADE **A** and with LBE **B**. Resulting fit parameters and percentage of dissociated complex at 1100 µm explosion width are given in **Supplementary Table 2**.

## Supplementary Tables

**Supplementary Table 1: DNA Sequences**
Assigned name and strand of DNA Sequences as well as their binding partner. Each DNA pair consist of a 35mer and a smaller strand.

| Name | Sequence (5' to 3') | Binding Partner |
|---|---|---|
| 9mer (B) | CCG TAA TCT | 35mer (B) |
| 10mer (A) | TAC TAA AAA C | 35mer (A) |
| 10mer (B) | CGT AAT CTC A | 35mer (B) |
| 11mer (A) | CAT AAT CAA CT | 35mer (A) |
| 15mer (A) | TAC TAA AAA CAT AAT | 35mer (A) |
| 15mer (B) | CTC AAA AAA ACT ACA | 35mer (A) |
| 35mer (A) | ATT GTA GTT TTT TTG AGT TGA TTA TGT TTT TAG TA | |
| 35mer (B) | TTT TGT GAG ATT ACG GAA CCT TTT TTT TTT TTT GT | |

**Supplementary Table 2: Linear Fit Results from dissociation curves**

Resulting fit parameters, the corresponding percentage of dissociated bond at an explosion width of 1100 µm and reference $K_D$ values for the systems used. DNA affinities are taken from (Young *et al.*, 2020), ROQ with ADE and LBE from (Tants *et al.*, 2022) and (Essig *et al.*, 2018) respectively.

| System | Slope | y-Intercept | mean % dissociated bond at 1100 µm | ref. $K_D$ / nM |
|---|---|---|---|---|
| 9mer (B) + 35mer (B) | 0.032 ± 0.003 | 32.5 ± 1.7 | **62.6 ± 4.8** | **2050** |
| | 0.012 ± 0.003 | 44.3 ± 2.7 | | |
| 10mer (A) + 35mer (A) | 0.0228 ± 0.0016 | 50.4 ± 1.2 | **75.1 ± 0.5** | **3720** |
| | 0.0172 ± 0.0014 | 55.8 ± 1.1 | | |
| 10mer (B) + 35mer (B) | 0.0389 ± 0.003 | 13.8 ± 2.9 | **58.6 ± 2.2** | **907** |
| | 0.0164 ± 0.0018 | 42.6 ± 1.4 | | |
| 11mer (A) + 35mer (A) | 0.018 ± 0.003 | 50.1 ± 2.2 | **66.4 ± 3.7** | **241** |
| | 0.0100 ± 0.0011 | 51.6 ± 0.9 | | |
| 15mer (A) + 35mer (A) | 0.031 ± 0.004 | 13.1 ± 3.0 | **41.8 ± 4.1** | **31** |
| | 0.0134 ± 0.0017 | 23.4 ± 1.4 | | |
| | 0.0210 ± 0.0017 | 16.8 ± 1.4 | | |
| 15mer (B) + 35mer (A) | 0.026 ± 0.002 | 9.1 ± 1.8 | **37.7 ± 0.4** | **3.5** |
| | 0.024 ± 0.002 | 11.3 ± 1.9 | | |
| ROQ + ADE | 0.024 ± 0.003 | 29 ± 3 | **58.5 ± 2.3** | **232** |
| | 0.0223 ± 0.0017 | 36.2 ± 1.6 | | |
| ROQ + LBE | 0.020 ± 0.016 | 59.3 ± 14.8 | **77.0 ± 4.9** | **3600** |
| | 0.055 ± 0.030 | 11.3 ± 29.7 | | |